© 2018. Published by The Company of Biologists Ltd | Journal of Cell Science (2018) 131, jcs210179. doi:10.1242/jcs.210179

SHORT REPORT

Feedback regulation by antagonistic epigenetic factors potentially maintains developmental homeostasis in *Drosophila*

Devendran A. Sadasivam and Der-Hwa Huang*

ABSTRACT

Drosophila Polycomb group (PcG) repressors confer epigenetically heritable silencing on key regulatory genes through histone H3 trimethylation on lysine 27 (H3K27me3). How the silencing state withstands antagonistic activities from co-expressed trithorax group (trxG) activators is unclear. Upon overexpression of Trx H3K4 methylase, to perturb the silenced state, we find a dynamic process triggered in a stepwise fashion to neutralize the inductive impacts from excess Trx. Shortly after Trx overexpression, there are global increases in H3K4 trimethylation and RNA polymerase II phosphorylation, marking active transcription. Subsequently, these patterns diminish at the same time as the levels of Set1, an abundant H3K4 methylase involved in productive transcription, reduce. Concomitantly, the global H3K27me3 level is markedly reduced, corresponding to an increase in the amount of Utx demethylase. Finally, excess Pc repressive complex 1 (PRC1) is induced and located to numerous ectopic chromosomal sites independently of H3K27me3 and several key recruitment factors. The observation that PRC1 becomes almost completely colocalized with Trx suggests new aspects of recruitment and antagonistic interaction. We propose that these events represent a feedback circuitry ensuring the stability of the silenced state.

KEY WORDS: TrxG, PcG, Histone methylation, *Drosophila*

INTRODUCTION

A myriad of epigenetic factors, defined initially in *Drosophila* as the Polycomb group (PcG) repressors and trithorax group (trxG) activators (Jürgens, 1985; Kennison and Tamkun, 1988), act antagonistically to lock the on-off state of Hox and key developmental genes (Lanzuolo and Orlando, 2012; Simon and Kingston, 2013; Steffen and Ringrose, 2014). These factors are highly conserved in metazoans and play critical roles in development, cell pluripotency and carcinogenesis (Loubiere et al., 2016; Piunti and Shilatifard, 2016).

Studies of PcG proteins have revealed that they form two major multiprotein complexes acting cooperatively to mark and assemble Pc response elements (PREs) and surrounding genes into transcriptionally silent chromatin. Notably, Pc repressive complex 2 (PRC2) catalyzes trimethylation of H3 on K27 (H3K27me3), creating unique chromatin domains over PREs (Cao et al., 2002; Czermin et al., 2002; Müller et al., 2002). However, the exact mechanism responsible for the initial recruitment of PRC1/2 complexes to PREs remains elusive. Several common motifs have been identified in PREs, including GA and TG dinucleotide repeats and binding sites for Pleiohomeotic (Pho) and Pho-like (Fritsch et al., 1999; Horard et al., 2000; Huang et al., 2002; Schwendemann and Lehmann, 2002; Brown and Kassis, 2010; Ray et al., 2016). Although these motifs and related factors are critical for the activity of a specific set of PREs, their contributions to the global recruitment of PRC1/2 have not been established.

Another important question is how the silenced state can be sustained in the presence of ubiquitously expressed trxG proteins, which have antagonistic activities. Several distinct activities have been described for trxG proteins, including histone methylation (Byrd and Shearn, 2003; Shilatifard, 2012), chromatin remodeling (Kingston and Tamkun, 2014) and modulation of transcription elongation (Yang et al., 2005; Devaiah et al., 2012). Importantly, the supply of extra dosages of trxG proteins by overexpression can disrupt the silenced state, resulting in the ectopic expression of Hox genes (Chang et al., 2007; Sadasivam and Huang, 2016). These activated Hox genes may return rapidly to the silenced state after Trx withdrawal, and the effective erasure of the active state is dependent upon PcG and other epigenetic factors (Sadasivam and Huang, 2016). Thus, a mechanism that can survey and restore the proper balance between PcG and trxG proteins seems to be necessary to ensure stable transmission of the silenced state.

To explore the potential mechanism, we used overexpression of Trx H3K4 methylase to perturb the genome and monitored progressive changes on RNA Polymerase II (RNAPII), chromatin landscapes and various epigenetic factors. We found that these factors are dynamically modulated. Moreover, excess PRC1 is induced, showing almost complete overlap with Trx. These results reveal a feedback process preventing long-term global perturbation triggered by Trx overexpression.

RESULTS AND DISCUSSION

We have previously shown that overexpression of the Trx H3K4 methylase in imaginal discs induces phosphorylation of RNAPII and altered histone modifications on Hox genes, resulting in ectopic Hox expression and aberrant adult appendages (Sadasivam and Huang, 2016). We anticipated that similar changes might occur globally, allowing us to determine various responses at the epigenomic and transcriptomic levels. Thus, we monitored the global patterns of RNAPII, histone modifications and several epigenetic factors on polytene chromosomes from the salivary glands of dpp^{blk}-*Gal4*; *UAS-trx* flies (hereafter termed *dpp*>Trx) (Brand and Perrimon, 1993), by performing co-staining with BEAF-32, which marks boundary elements, as an internal control (Zhao et al., 1995). Despite large increases of Trx RNA and protein (Fig. S1A), no obvious changes were seen on chromosomes from the *dpp*>Trx flies for two major phosphorylated isoforms of RNAPII (i.e. at S5 and S2), marking transcriptionally active RNAPII (Zhou et al., 2012; Heidemann et al., 2013), indicating that there is no global increase of transcription (Fig. S1B). We further

Institute of Molecular Biology, Academia Sinica, Taipei, Taiwan 11529.

*Author for correspondence (mbdhuang@ccvax.sinica.edu.tw)

D.A.S., 0000-0003-3109-9739; D.-H.H., 0000-0003-2679-0867

Received 26 August 2017; Accepted 4 April 2018

Journal of Cell Science (2018) 131, jcs210179. doi:10.1242/jcs.210179

examined the pattern of H3K27 acetylation and H3K36 methylation, which are often associated with active transcription (Simon and Kingston, 2013). Consistent with the lack of global transcriptional activation, we did not detect significant increases of these modifications on chromosomes from the *dpp*>Trx flies (Fig. S1C,D). Surprisingly, excess Trx failed to induce global increases in H3K4 mono-, di- or tri-methylation (Fig. S1E), despite its function as an H3K4 methylase (Shilatifard, 2012). These unexpected results suggest the involvement of a previously unknown process.

To resolve this puzzle, we examined the patterns of two additional *Drosophila* H3K4 methylases, Trx-related (Trr) and Set1. Since their mammalian homologs, like Trx, belong to the COMPASS family of methylase complexes (Shilatifard, 2012), the fluctuation of these factors may affect the global patterns of H3K4 methylation. The level of Trr was not affected by *dpp*>Trx (Fig. S1F); however, there was a marked reduction of Set1 (Fig. 1A,D). Set1 has been reported to be the major H3K4 methylase in *Drosophila* cells and is directly linked to productive transcription (Ardehali et al., 2011; Mohan et al., 2011). Conceivably, Set1 reduction may abrogate the effect of *dpp*>Trx on global H3K4 methylation and active transcription.

Our earlier studies also showed that there is a modest reduction of H3K27me3 on Hox genes in *dpp*>Trx imaginal tissues (Sadasivam and Huang, 2016). In gland cells, global levels of H3K27me3 were substantially reduced (Fig. 1B,E). Since PRC2 is the only enzyme known to catalyze the production of H3K27me3 in *Drosophila* (Cao et al., 2002; Czermin et al., 2002; Müller et al., 2002), we measured the RNA levels of its four core subunits. Surprisingly, there was little change for E(z), Su(z)12, Esc and Nurf55 (also known as Caf1-55) in *dpp*>Trx gland cells compared to wild type (Fig. 1F), suggesting that PRC2 is not involved in H3K27me3 reduction. Since the level of H3K27me3 might also be affected by a demethylase, we examined the level of the H3K27me3-specific demethylase Utx (Smith et al., 2008). Remarkably, high levels of Utx were induced by *dpp*>Trx (Fig. 1C,G). The reciprocal profile of Utx and H3K27me3 strongly suggests a direct link between them.

H3K27me3 generally marks silenced chromatin. In addition, it is believed to tether PRC1 through the chromodomain of Pc (Cao et al., 2002; Fischle et al., 2003; Min et al., 2003), which constitutes the key feature of the epigenetically heritable mechanism. The reduction of H3K27me3 raised a question about the status of PRC1. In contrast to the constant level of PRC2, excess PRC1 was induced by *dpp*>Trx (Fig. 2A; Fig. S2A). On chromosomes from *dpp*>Trx flies, signals for the core subunits of PRC1 (Francis et al., 2001), including Pc, Psc and Ph, emerged at many new sites, and the pairs of Psc/Pc or Psc/Ph showed mutual colocalization at these sites (Fig. 2B; Fig. S2B), supporting the integrity of PRC1. However, the majority of these sites clearly lacked H3K27me3 (Fig. 2C), indicating that the recruitment of newly induced PRC1 is independent of H3K27me3. Similarly, PRC1 has been previously identified in regions without H3K27me3 marks (Schaaf et al., 2013; Loubiere et al., 2016). We note that some of these new sites might result from elevated PRC1 binding to regions with low PRC1 before *dpp*>Trx.

Since these PRC1 complexes might be recruited by DNA-binding factors, we further examined the involvement of GAGA factor (Gaf, also known as Trl), Pipsqueak (Psq), Combgap (Cg) and Pho (Fritsch et al., 1999; Horard et al., 2000; Huang et al., 2002; Ray et al., 2016), which have been frequently implicated in recruitment. The global distribution patterns of Psc and these factors were examined. As observed for chromosomes in wild-type (WT) flies, less than half of Psc signal was colocalized with Gaf, Psq or Cg on chromosomes from the *dpp*>Trx flies (Fig. S2C), indicating that they are not determinants for recruiting new PRC1. Interestingly, extensive colocalization (>95%) was observed for Psc and Pho on

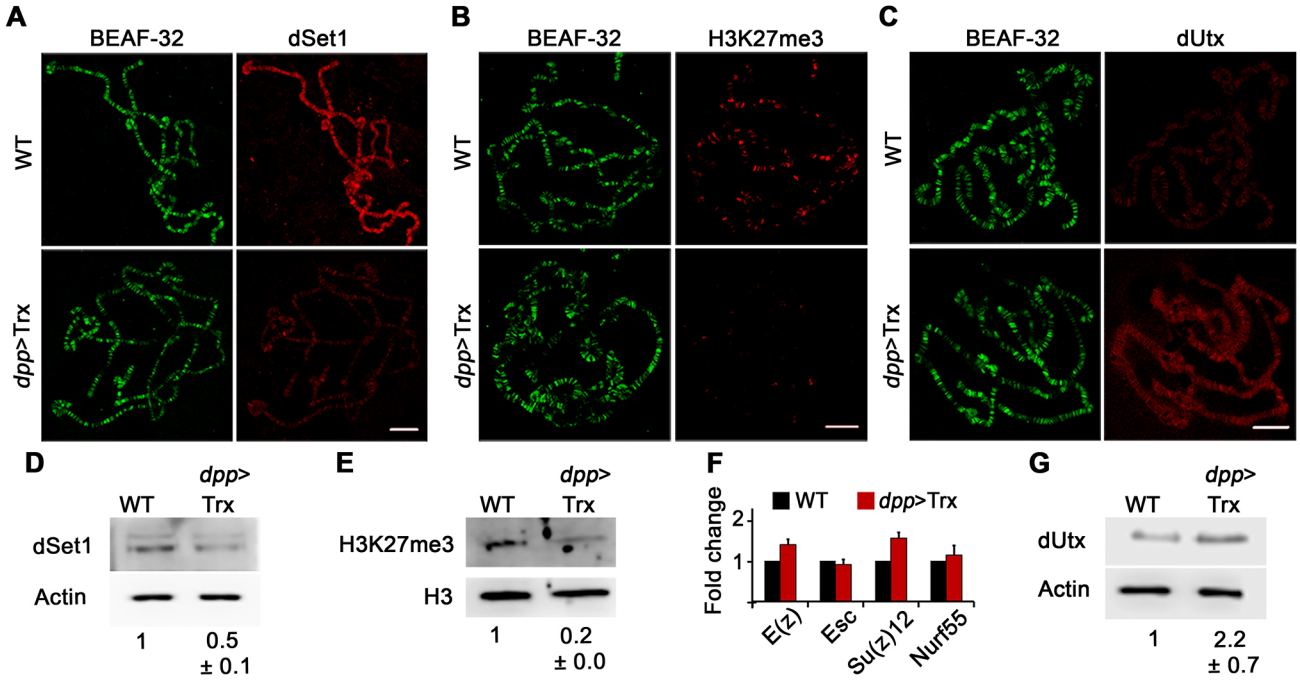

Fig. 1. Modulation of epigenetic factors upon *dpp*>Trx. (A–C) Staining of epigenetic factors (red) and BEAF-32 control (green) are shown for chromosomes from WT (upper panels) and *dpp*>Trx (lower panels) flies. Set1 (dSet1, A), H3K27me3 (B) and Utx (dUtx, C) were examined. (D–G) Relative abundance of epigenetic factors in gland cells was measured by western blotting (D,E,G) or quantitative PCR (F), using actin (D,E,G) or Rpl32 (F) as controls for normalization. The levels of various factors relative to WT samples are indicated as the mean±s.d., *n*=3 (D,F,G), *n*=2 (E). Scale bars: 20 µm.

Journal of Cell Science (2018) 131, jcs210179. doi:10.1242/jcs.210179

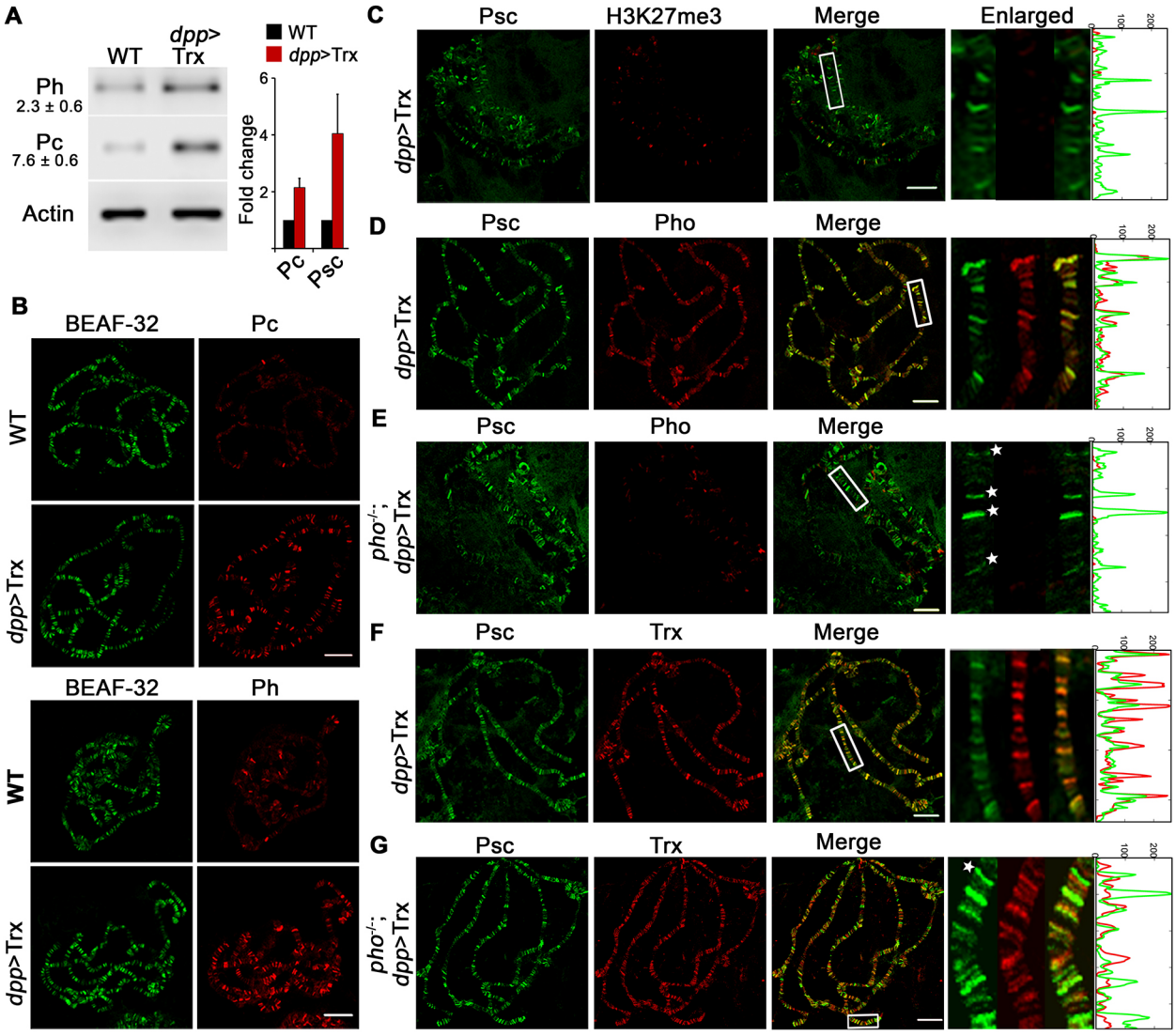

Fig. 2. Induction and recruitment of PRC1 upon *dpp*>Trx. (A) Induction of PRC1 core subunits in gland cells. The amounts of Ph/Pc/Actin or Pc/Psc/Rpl32 were measured by western blotting (left) or quantitative PCR (right), respectively. Their relative abundance is indicated as the mean±s.d. (*n*=3). (B) The distribution of Pc or Ph (red) is shown on chromosomes from WT (upper panels) and *dpp*>Trx (lower panels) flies with BEAF-32 controls (green). (C) Lack of global colocalization between PRC1 and H3K27me3 on chromosomes from *dpp*>Trx flies. Staining of Psc (red) and H3K27me3 (green) on chromosomes from *dpp*>Trx flies are shown as separate and merged images. An enlarged view of the boxed section is also shown, together with plots showing relative intensity of each signal. (D,E) Distribution of Psc and Pho on chromosomes from *dpp*>Trx flies in WT (D) or pho^{1} ($pho^{-/-}$) backgrounds (E). Separate, merged and enlarged images of Psc (green) and Pho (red) staining are shown as in C. Four Psc sites without discernible Pho signals are indicated (stars). Residual Pho staining on pho^{1} mutant chromosomes may arise from cross-reactivity to Pho-like (Brown et al., 2003). (F,G) Distributions of Psc (green) and Trx (red) on *dpp*>Trx chromosomes in WT (F) or pho^{1} backgrounds (G) are shown. A rare example of a Psc site without Trx is indicated (star). Scale bars: 20 µm.

chromosomes from the *dpp*>Trx flies (Fig. 2D). However, the level of chromosome-associated Psc signal was not significantly affected by a pho^{1} mutation. The presence of Psc bands without discernible Pho signals on mutant chromosomes strongly suggests that Pho is not obligatory for recruiting induced PRC1 during larval stages (Fig. 2E). Although these results do not exclude the possibility that a combination of multiple factors is involved in recruitment, they suggest that other mechanisms may exist. Given that 30–50% of Trx sites overlap with PRC1 sites on WT chromosomes (Chinwalla et al., 1995; Schuettengruber et al., 2009), we further examined their distributions on chromosomes from *dpp*>Trx flies. Strikingly, almost complete concurrence was observed for Trx and Psc (Fig. 2F), although their relative intensities varied occasionally. Importantly, this pattern was almost unaffected by pho^{1} mutation (Fig. 2G). Thus, Trx appears to be involved in a novel mechanism for recruiting new PRC1. Regardless of its exact nature, our finding strongly supports an alternative model for recruitment.

Because the *dpp-Gal4* driver is continuously active in glands from the embryonic stage onwards (Staehling-Hampton et al., 1994), dynamic changes induced transiently during early development might escape detection at later stages. Thus, we adopted a strategy to allow conditional induction of *dpp*>Trx by introducing the constitutively expressed temperature-sensitive Gal4 inhibitor $Gal80^{ts}$ (McGuire et al., 2004). Following temperature upshift for different periods (Fig. 3A), we monitored progressive changes of various factors. By 24 h, H3K27me3 signals dropped to levels similar to those observed for continuous *dpp*>Trx (Fig. 3B). In parallel, high levels of Utx were induced (Fig. 3C). This reciprocity supports a causal relationship between them. However, Pc induction appeared to lag behind, requiring an additional 24 h to

Journal of Cell Science (2018) 131, jcs210179. doi:10.1242/jcs.210179

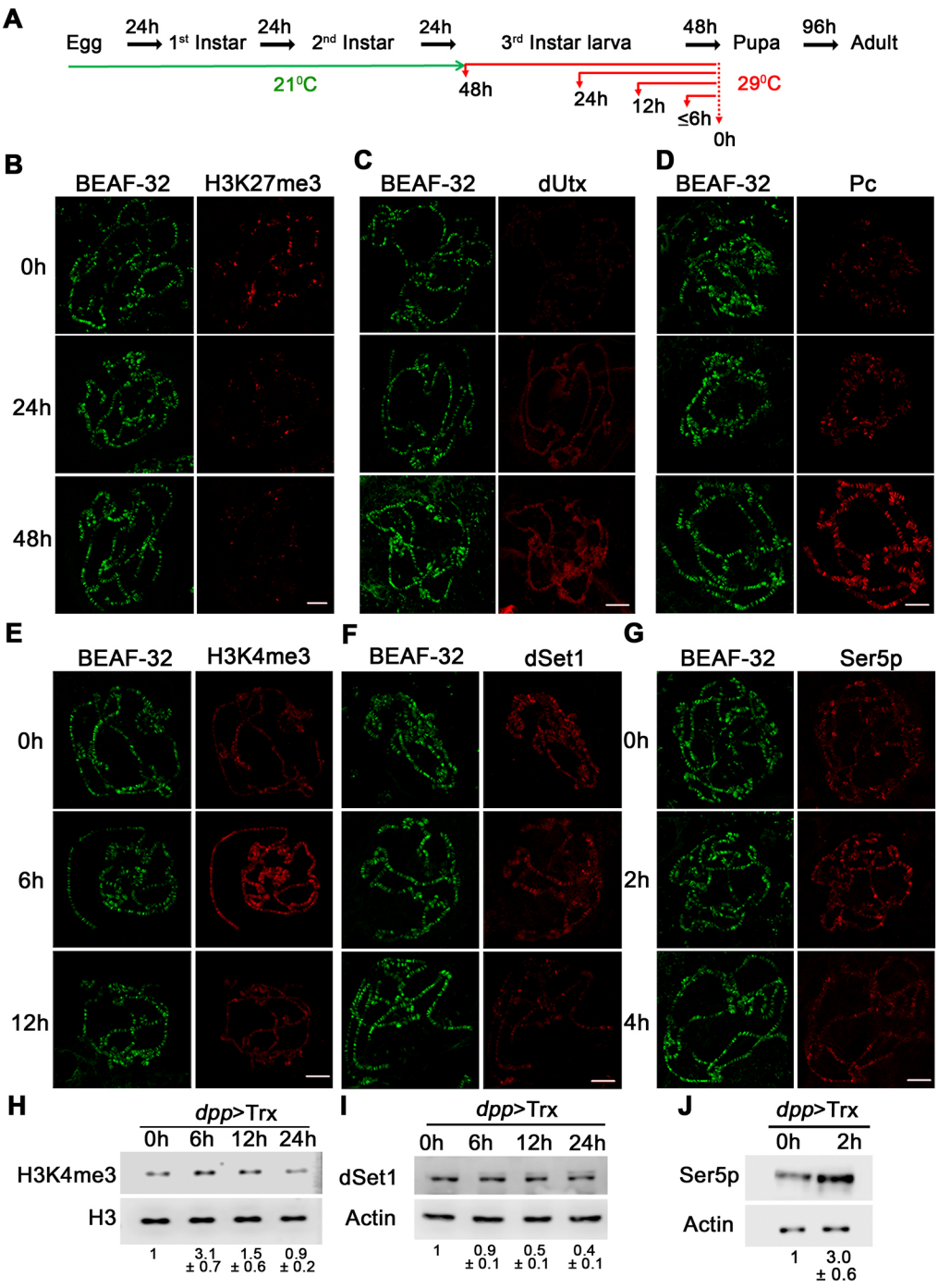

Fig. 3. Dynamic regulation of epigenetic factors. (A) Scheme for inactivation of Gal80^{ts} by temperature upshift during larval development (red line). (B–G) The effects of *dpp*>Trx on H3K27me3 (B), Utx (dUtx, C), Pc (D), H3K4me3 (E), Set1 (dSet1, F) and RNAPII phosphorylated at S5 (Ser5p, G) were monitored at 0–48 h (B–D), 0–12 h (E,F) or 0–4 h (G) after Gal80^{ts} inactivation. Staining of epigenetic factors (red) and BEAF-32 control (green) is shown. (H–J) Gland extracts after 0–24 h (H, I) and 0–2 h (J) of *dpp*>Trx induction were probed for H3K4me3 (H), Set1 (I), Ser5p (J) and Actin. Their relative abundance (mean ±s.d.) is indicated (*n*=2). Scale bars: 20 µm.

reach maximal levels (Fig. 3D). Thus, these events occur in a sequential order.

As the major H3K4 methylase (Ardehali et al., 2011; Mohan et al., 2011), a reduction in the amount of Set1 could interfere with the effect of *dpp*>Trx on global levels of H3K4 methylation or active RNAPII. Thus, we re-examined the H3K4 methylation or active RNAPII signals in response to a shorter interval of *dpp*>Trx. Interestingly, H3K4me3 showed a substantial increase by 6 h at the expense of H3K4me1, followed by a sharp decline after another 6 h (Fig. 3E,H; Fig. S2D). A pronounced Set1 reduction was also observed during this interval (Fig. 3F,I). Again, the concomitant reduction of H3K4me3 and its predominant methylase supports a causal relationship. In addition, these results strongly suggest that Trx is capable of catalyzing tri-methylation of H3K4 *in vivo* rather than merely mono-methylation (Tie et al., 2014).

During this 12 h timeframe, we still failed to detect significant changes in RNAPII (Fig. S2E). Thus, we conducted experiments with even shorter periods of *dpp*>Trx induction. An increase of active RNAPII with phosphorylation on S5 or S2 was evident by 2 h. However, these patterns diminished rapidly by 4 h (Fig. 3G,J; Fig. S2F). Thus, the global effects on H3K4me3 and transcription are rather dynamic, even under continuous supply of Trx. The relative levels of various epigenetic factors induced by Trx overexpression are summarized in Fig. 4A. Remarkably, profiles of these factors appear to be most dynamic during the initial 12 h. Importantly, the effects on H3K4me3 and active RNAPII can be

Journal of Cell Science (2018) 131, jcs210179. doi:10.1242/jcs.210179

A

		Early		Intermediate			Late	
	0h	2h	4h	6h	12h	24h	48h	L3
H3K4me3	+[1,2]	++[1]	-	+++[1,2]	+[1,2]	+[1,2]	-	+[1]
H3K4me1	+++[1,2]	+++[1]	-	+[1,2]	+++[1,2]	+++[1,2]	-	+++[1]
RNAPII	+[1,2]	++[1,2]	+[1]	+[1,2]	+[1,2]	+[1]	-	+[1]
dSet1	+++[1,2]	-	-	+++[1,2]	+[1,2]	+[1,2]	-	+[1,2]
H3K27me3	+++[1,2]	-	-	-	-	+[1]	+[1]	+[1,2]
dUtx	+[1,2]	-	-	+[2]	++[2]	++[1,2]	+++[1]	+++[1,2]
Pc	+[1,2]	-	-	-	-	++[1]	+++[1]	+++[1,2]

1, Polytene staining; *2*, Western blot; -, not done

B

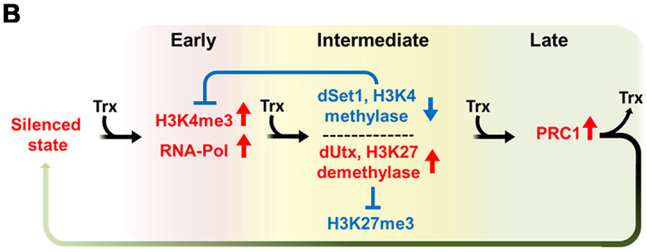

Fig. 4. Feedback regulation for the maintenance of homeostasis. (A) Fluctuations in various factors relative to the non-induced state (0 h) is indicated by the number of '+' signs for early (2–4 h), intermediate (6–24 h) and late phases (>24 h). Continuous expression to the third-larval instar is indicated as L3. Estimates are based on chromosomal staining (*1*) or western blotting (*2*). -, not done. (B) Feedback model. In the early phase, Trx overexpression causes global increases of H3K4me3 and active RNAPII. The reduction of Set1 (dSet1) compromises these effects in intermediate phase. Concurrently, increased Utx (dUtx) levels result in a reduction in the amount of H3K27me3. In the late phase, excess PRC1 is induced and recruited to Trx-containing sites. Following the withdrawal of *dpp*>Trx, epigenetic factors return quickly to the original states, thereby erasing the effects induced by Trx overexpression. Note that the arrows do not imply direct induction or repression by Trx.

reversed even in the presence of excess Trx. From 12 h to 24 h, relatively constant profiles are established. We note that Trx is associated with the promoter of Utx and PRC1 subunits (Schuettengruber et al., 2009). Whether these genes are directly upregulated by Trx awaits further analyses.

To examine the persistence of these effects, we next monitored their changes after the interruption of Trx overexpression by lowering the growth temperature to produce active Gal80 (Fig. S3A). By 24 h, Utx declined to its original levels (Fig. S3B). In contrast, levels of H3K27me3 began to rise by 12 h and fully recovered by 24 h (Fig. S3C). Concomitantly, Pc levels were reduced to their original levels (Fig. S3D). These results strongly suggest that epigenetic effects induced by *dpp*>Trx are reversible.

To test whether diploid somatic cells can also respond to *dpp*>Trx, we examined the level of Pc and Ph in imaginal discs. Unlike polyploid gland cells, rather modest increases of Pc and Ph were seen along the anteroposterior border of wing discs with an active *dpp*-Gal4 driver (Fig. S4A), presumably due to much lower genome copy (i.e. 2N versus ∼1000N) and shorter duration of *dpp*>Trx activity in these cells. To further substantiate these findings, we measured the level of Pc and Ph in entire discs with a ubiquitous driver (i.e. *Act*-Gal4) (Fig. S4B). Indeed, significant increases were observed for both factors, indicating that similar responses occur in both polyploid and diploid cells.

Our studies have revealed a stepwise process in which several functionally opposing epigenetic factors are dynamically modulated. These events are tentatively divided into three phases (Fig. 4B). In the early phase, a high dose of Trx triggers the genome-wide conversion of H3K4me1 and/or H3K4me2 into H3K4me3, leading to increased phosphorylation of RNAPII and productive transcriptional elongation. Subsequently, these effects are mostly diminished in the intermediate phase, with a concomitant reduction in the predominant methylase Set1. In addition, an increase in the amount of the Utx demethylase results in the removal of H3K27me3, a landmark of the silenced domain. In the late phase, excess PRC1 is induced and recruited to a large number of chromosomal sites independently of H3K27me3 and several key PRE-binding factors. Interestingly, these sites are already occupied by Trx, implying that there is a different mode of PRC1 recruitment. Although the exact role of Trx in recruiting newly induced PRC1 remains to be determined, it is conceivable that Trx acts as a critical component of this novel mechanism. Given its ability to mediate the compaction of nucleosome arrays (Francis et al., 2004), and its established role in transcriptional silencing, we speculate that newly recruited PRC1 may further block Trx activity in the late phase to facilitate the rapid recovery to the original state. Consistent with this idea, we have found that Trx-induced Hox gene expression returns to the silent state when extra Trx is no longer provided and that the effectiveness of this process is compromised in cells with reduced PRC1 levels (Sadasivam and Huang, 2016). We note that PRC1 is also associated with active genes without H3K27me3 marks (Schaaf et al., 2013; Venkatesh and Workman, 2015). However, the belated appearance of PRC1 at the stage when most active marks have already receded argues against a role in gene activation during this process. We suggest that this series of events constitutes a feedback loop that is triggered when the balance between PcG and trxG proteins is adversely perturbed. Once induced, this mechanism can prevent persistent and drastic perturbations on epigenome and transcriptome, thereby maintaining their stability. We propose that this feedback mechanism can insure the transmission of developmental potential of undifferentiated cells.

MATERIALS AND METHODS

Fly stocks

P(GSV6)GS12194/TM3 (UAS-trx) was obtained from the *Drosophila* Genetic Resource Center (DGRC), Kyoto, Japan. *w;dpp^{blk}-Gal4/TM3*, *Act-Gal4/TM3*, and *tub-Gal80^{ts}/CyO* were obtained from the Bloomington *Drosophila* Stock Center (BDSC), Bloomington, IN. *pho^{1}/Act-GFP* was a gift from Judy Kassis (NICHD, NIH, USA).

Genetic crosses

Flies were raised at 25°C on standard food unless otherwise mentioned. Homozygous *UAS-trx* virgin females were crossed to *dpp^{blk}-Gal4/TM6B,Tb* males and *dpp^{blk}-Gal4/UAS-trx* were identified by their non-*tubby* status or by GFP expression. Staining in the *pho^{1}* mutant background was performed by crossing the *pho^{1}* heterozygous mutant carrying *UAS-trx* with a *pho^{1}* heterozygous mutant carrying *dpp*-Gal4. *pho^{1}* homozygous mutants were identified as described previously (Brown et al., 2003). For the experiments described in Fig. 3A and Fig. S3A, virgin females carrying *UAS-trx* were crossed to *tub-Gal80^{ts};dpp-Gal4* males and kept at either 29°C or 21°C for indicated periods to inactivate or activate Gal80^{ts}, respectively.

Immunostaining and immunoblotting

For polytene chromosome staining, salivary glands were dissected from third-instar larvae, fixed,and squashed as described previously (Chang et al., 2001). The details of primary and secondary antibody dilutions are described in a separate section below. DNA was stained with Hoechst 33258 (0.25 µg/ml). All confocal images were taken using an LSM510Meta microscope (Zeiss) with a 63× objective lens. Images were aligned and processed using Adobe Photoshop CS3. The scale bar in all confocal images

is 20 µm. Chromosomes from WT and *dpp*>Trx samples and time-course experiments were stained and imaged at the same time with the same exposure. Experiments were performed between two and four times and ∼30–50 nuclei were examined in each case. Figures show representative results. In colocalization studies, signal intensity graphs were plotted from enlarged images using ImageJ (NIH). For imaginal tissue staining, wing imaginal discs from WT or *dpp*>Trx third-instar larvae were fixed with 3.7% formaldehyde in PBS for 20 min. Discs were washed, blocked and incubated with primary and secondary antibodies as described previously (Chang et al., 2001; Sadasivam and Huang, 2016). DNA was stained with Hoechst 33258 (0.25 µg/ml). Images were taken using an LSM510Meta microscope (Zeiss) with a 40× objective lens. Images were aligned and processed using Adobe Photoshop CS3.

For western blot analysis, imaginal tissues or salivary glands collected from WT and *dpp*>Trx larvae were lysed in SDS-Urea buffer. Extracts were separated by 8% or 15% SDS-PAGE and blotted onto nitrocellulose filters. After protein transfer, the membranes were treated with the blocking buffer followed by incubation with primary and secondary antibodies. A LI-COR Bioscience system was used for image acquisition. The fold-change compared to WT, and standard deviations from two or three independent blots are indicated.

Antibodies

Antibodies against the following proteins were obtained from the following sources: BEAF-32 and Psc from Developmental Studies Hybridoma Bank; Cg and Pho from Judy Kassis (Brown et al., 2003; Ray et al., 2016); Trx, Trr, Utx, Set1 from Ali Shilatifard (Department of Biochemistry and Molecular Genetics, Northwestern University, USA) (Herz et al., 2012); Psq from Celeste Berg (Department of Genome Sciences, University of Washington, USA) and affinity-purified as described previously (Horowitz and Berg, 1996; Huang et al., 2002); affinity-purified Gaf (Tsai et al., 2016), Pc and Ph (Chang et al., 2001); H3K4me3 from Abcam (ab8580); H3K4me2, H3K4me1 and H3K27ac from Upstate (07-030, 07-436 and 07-360, respectively); H3K27me3 and H3 from Active Motif (39156 and 39163, respectively); RNA Polymerase II phosphorylated at S5 (H14) and S2 (H5) (denoted Ser5p and Ser2p) from Covance (MMS-134R and MMS-129R, respectively); and actin from Chemicon (MAB-1501).

Antibody dilutions

For polytene staining, antibodies were diluted as follows: BEAF-32, 1:50; Psc, 1:40; Pc, 1:1000; Ph, 1:200; Gaf, 1:500; Psq, 1:500; Cg, 1:500; Pho, 1:500; Trx, 1:200; Trr, 1:100; Utx, 1:200; Set1, 1:200; Ser5p, 1:50; Ser2p, 1:40; H3K4me3, 1:200; H3K4me2, 1:100; H3K4me1, 1:100; H3K27me3, 1:100; H3K27ac, 1:100. For western blots, antibodies were diluted as follows: Pc, 1:2000; Ph, 1:500; Utx, 1:3000; Set1, 1:500; H3K4me3, 1:500; H3K4me1, 1:500; H3K27me3, 1:500; Ser5p; 1:1000; Ser2p, 1:500; H3, 1:10,000; Actin, 1:15,000. For imaginal discs staining, the following dilutions were used: Pc, 1:1000; Ph, 1:500. Secondary antibodies were used at 1:200 for Cy5-conjugated goat anti-rabbit IgG, rhodamine-conjugated goat anti-mouse IgM (both from Jackson ImmunoResearch), or Alexa 488 goat anti-mouse IgG1 (Molecular Probes).

Quantitative real-time PCR analysis

Total RNAs from 20–40 wing discs or salivary glands were prepared from third-instar larvae of different genotypes by the RNeasy protocol (QIAGEN). After reverse transcription, cDNA levels were measured by quantitative PCR according to the vendor's protocol by using SYBR Green at standard settings (ABI 7500, Applied Bioscience). Three separate experiments (each in triplicate) were performed. The primers used are as follows: Rpl32 forward, 5′-ACTTCATCCGCCACCAGTCGG-3′, Rpl32 reverse, 5′-CGCTCGACAATCTCCTTGCGC-3′; Pc forward, 5′-GAGTAAGGGGAAGTTGGGGC-3′, Pc reverse, 5′-GTTTACCTCCGGTTCCCAGG-3′; Trx forward, 5′-TTTGCGTCCCTGGGTTTGAT-3′, Trx reverse, 5′-TCCAACCTAATAGTGGCGGC-3′; Psc forward, 5′-TCCGCACATCATCTGTCACC-3′, Psc reverse, 5′-CCCTTTTGCGCATCAGTTCC-3′; Esc forward, 5′-GCCAGGAGAGGTGAAGAGGT-3′, Esc reverse, 5′-AGAACCACGGAGCCAACATC-3′; Su(Z)12 forward, 5′-TGCACAAGAAGCAGGAAGACC-3′, Su(Z)12 reverse, 5′-CTGCCTCGTTTCAAATGAGCC-3′; Nurf55 forward, 5′-CCACACCCAAGGAGCATAGG-3′, Nurf55 reverse, 5′-GTGGCCAGAATGAACTCCGA-3′; and E(z) forward, 5′-CGGAGCGGATCAGTTTAAGCT-3′, E(z) reverse, 5′-TGCGCACCCTCCTTAAGAAAG-3′.

Acknowledgements

We thank J. Kassis, A. Shilatifard, the Developmental Studies Hybridoma Bank, Bloomington Stock Center for antibodies and fly stocks. We thank the IMB core facilities for technical help, J. Kung and M.-C. Yao for discussion, and J. O'Brien for editing assistance.

Competing interests

The authors declare no competing or financial interests.

Author contributions

Conceptualization: D.A.S., D.-H.H.; Methodology: D.A.S., D.H.; Formal analysis: D.A.S., D.-H.H.; Investigation: D.A.S.; Resources: D.A.S., D.-H.H.; Writing - original draft: D.-H.H.; Writing - review & editing: D.-H.H.; Funding acquisition: D.-H.H.

Funding

This research is funded by an intramural grant from Academia Sinica, Taiwan.

Supplementary information

Supplementary information available online at
http://jcs.biologists.org/lookup/doi/10.1242/jcs.210179.supplemental

References

Ardehali, M. B., Mei, A., Zobeck, K. L., Caron, M., Lis, J. T. and Kusch, T. (2011). *Drosophila* Set1 is the major histone H3 lysine 4 trimethyltransferase with role in transcription. *EMBO J.* **30**, 2817-2828.

Brand, A. H. and Perrimon, N. (1993). Targeted gene expression as a means of altering cell fates and generating dominant phenotypes. *Development* **118**, 401-415.

Brown, J. L. and Kassis, J. A. (2010). Spps, a *Drosophila* Sp1/KLF family member, binds to PREs and is required for PRE activity late in development. *Development* **137**, 2597-2602.

Brown, J. L., Fritsch, C., Müller, J. and Kassis, J. A. (2003). The *Drosophila* pho-like gene encodes a YY1-related DNA binding protein that is redundant with pleiohomeotic in homeotic gene silencing. *Development* **130**, 285-294.

Byrd, K. N. and Shearn, A. (2003). ASH1, a Drosophila trithorax group protein, is required for methylation of lysine 4 residues on histone H3. *Proc. Natl. Acad. Sci. USA* **100**, 11535-11540.

Cao, R., Wang, L. J., Wang, H. B., Xia, L., Erdjument-Bromage, H., Tempst, P., Jones, R. S. and Zhang, Y. (2002). Role of histone H3 lysine 27 methylation in Polycomb-group silencing. *Science* **298**, 1039-1043.

Chang, Y. L., Peng, Y. H., Pan, I. C., Sun, D. S., King, B. and Huang, D. H. (2001). Essential role of *Drosophila* Hdac1 in homeotic gene silencing. *Proc. Natl. Acad. Sci. USA* **98**, 9730-9735.

Chang, Y.-L., King, B., Lin, S.-C., Kennison, J. A. and Huang, D.-H. (2007). A double-bromodomain protein, FSH-S, activates the homeotic gene Ultrabithorax through a critical promoter-proximal region. *Mol. Cell Biol.* **27**, 5486-5498.

Chinwalla, V., Jane, E. P. and Harte, P. J. (1995). The Drosophila Trithorax protein binds to specific chromosomal sites and is co-localized with Polycomb at many sites. *EMBO J.* **14**, 2056-2065.

Czermin, B., Melfi, R., McCabe, D., Seitz, V., Imhof, A. and Pirrotta, V. (2002). *Drosophila* enhancer of Zeste/ESC complexes have a histone H3 methyltransferase activity that marks chromosomal Polycomb sites. *Cell* **111**, 185-196.

Devaiah, B. N., Lewis, B. A., Cherman, N., Hewitt, M. C., Albrecht, B. K., Robey, P. G., Ozato, K., Sims, R. J. and Singer, D. S. (2012). BRD4 is an atypical kinase that phosphorylates Serine2 of the RNA Polymerase II carboxy-terminal domain. *Proc. Natl. Acad. Sci. USA* **109**, 6927-6932.

Fischle, W., Wang, Y., Jacobs, S., Kim, Y., Allis, D. and Khorasanizadeh, S. (2003). Molecular basis for the discrimination of repressive methyl-lysine marks in histone H3 by Polycomb and HP1 chromodomains. *Genes Dev.* **17**, 1870-1881.

Francis, N. J., Saurin, A. J., Shao, Z. and Kingston, R. E. (2001). Reconstitution of a functional core Polycomb repressive complex. *Mol. Cell.* **8**, 545-556.

Francis, N. J., Kingston, R. E. and Woodcock, C. L. (2004). Chromatin compaction by a Polycomb group protein complex. *Science* **306**, 1574-1577.

Fritsch, C., Brown, J. L., Kassis, J. A. and Müller, J. (1999). The DNA-binding Polycomb group protein Pleiohomeotic mediates silencing of a *Drosophila* homeotic gene. *Development* **126**, 3905-3913.

Heidemann, M., Hintermair, C., Voss, K. and Eick, D. (2013). Dynamic phosphorylation patterns of RNA polymerase II CTD during transcription. *Bba-Gene Regul. Mech.* **1829**, 55-62.

Herz, H.-M., Mohan, M., Garruss, A. S., Liang, K., Takahashi, Y.-H., Mickey, K., Voets, O., Verrijzer, C. P. and Shilatifard, A. (2012). Enhancer-associated H3K4 monomethylation by Trithorax-related, the *Drosophila* homolog of mammalian Mll3/Mll4. *Genes Dev.* **26**, 2604-2620.

Horard, B., Tatout, C., Poux, S. and Pirrotta, V. (2000). Structure of a Polycomb response element and in vitro binding of Polycomb group complexes containing GAGA factor. *Mol. Cell Biol.* **20**, 3187-3197.
Horowitz, H. and Berg, C. A. (1996). The *Drosophila* pipsqueak gene encodes a nuclear BTB-domain-containing protein required early in oogenesis. *Development* **122**, 1859-1871.
Huang, D.-H., Chang, Y.-L., Yang, C.-C., Pan, I. C. and King, B. (2002). pipsqueak encodes a factor essential for sequence-specific targeting of a Polycomb group protein complex. *Mol. Cell Biol.* **22**, 6261-6271.
Jürgens, G. (1985). A group of genes controlling the spatial expression of the bithorax complex in *Drosophila*. *Nature* **316**, 153-155.
Kennison, J. A. and Tamkun, J. W. (1988). Dosage-dependent modifiers of Polycomb and Antennapedia mutations in *Drosophila*. *Proc. Natl. Acad. Sci. USA* **85**, 8136-8140.
Kingston, R. E. and Tamkun, J. W. (2014). Transcriptional regulation by trithorax-group proteins. *Csh Perspect Biol.* **6**, a019349.
Lanzuolo, C. and Orlando, V. (2012). Memories from the Polycomb group proteins. *Annu. Rev. Genet.* **46**, 561-589.
Loubiere, V., Delest, A., Thomas, A., Bonev, B., Schuettengruber, B., Sati, S., Martinez, A.-M. and Cavalli, G. (2016). Coordinate redeployment of PRC1 proteins suppresses tumor formation during *Drosophila* development. *Nat. Genet.* **48**, 1436-1442.
McGuire, S. E., Mao, Z. and Davis, R. L. (2004). Spatiotemporal gene expression targeting with the TARGET and gene-switch systems in *Drosophila*. *Sci. STKE* **2004**, pl6.
Min, J., Zhang, Y. and Xu, R.-M. (2003). Structural basis for specific binding of Polycomb chromodomain to histone H3 methylated at Lys 27. *Genes Dev.* **17**, 1823-1828.
Mohan, M., Herz, H.-M., Smith, E. R., Zhang, Y., Jackson, J., Washburn, M. P., Florens, L., Eissenberg, J. C. and Shilatifard, A. (2011). The COMPASS family of H3K4 methylases in *Drosophila*. *Mol. Cell Biol.* **31**, 4310-4318.
Müller, J., Hart, C. M., Francis, N. J., Vargas, M. L., Sengupta, A., Wild, B., Miller, E. L., O'Connor, M. B., Kingston, R. E. and Simon, J. A. (2002). Histone methyltransferase activity of a *Drosophila* Polycomb group repressor complex. *Cell* **111**, 197-208.
Piunti, A. and Shilatifard, A. (2016). Epigenetic balance of gene expression by Polycomb and COMPASS families. *Science* **352**, aad9780.
Ray, P., De, S., Mitra, A., Bezstarosti, K., Demmers, J. A. A., Pfeifer, K. and Kassis, J. A. (2016). Combgap contributes to recruitment of Polycomb group proteins in *Drosophila*. *Proc. Natl. Acad. Sci. USA* **113**, 3826-3831.
Sadasivam, D. A. and Huang, D.-H. (2016). Maintenance of tissue pluripotency by epigenetic factors acting at multiple levels. *PLoS Genet.* **12**, e1005897.
Schaaf, C. A., Misulovin, Z., Gause, M., Koenig, A., Gohara, D. W., Watson, A. and Dorsett, D. (2013). Cohesin and Polycomb proteins functionally interact to control transcription at silenced and active genes. *PLoS Genet.* **6**, e1003560.
Schuettengruber, B., Ganapathi, M., Leblanc, B., Portoso, M., Jaschek, R., Tolhuis, B., van Lohuizen, M., Tanay, A. and Cavalli, G. (2009). Functional anatomy of Polycomb and trithorax chromatin landscapes in *Drosophila* embryos. *PLoS Biol.* **7**, e13.
Schwendemann, A. and Lehmann, M. (2002). Pipsqueak and GAGA factor act in concert as partners at homeotic and many other loci. *Proc. Natl. Acad. Sci. USA* **99**, 12883-12888.
Shilatifard, A. (2012). The COMPASS Family of histone H3K4 methylases: mechanisms of regulation in development and disease pathogenesis. *Annu. Rev. Biochem.* **81**, 65-95.
Simon, J. A. and Kingston, R. E. (2013). Occupying chromatin: Polycomb mechanisms for getting to genomic targets, stopping transcriptional traffic, and staying put. *Mol. Cell* **49**, 808-824.
Smith, E. R., Lee, M. G., Winter, B., Droz, N. M., Eissenberg, J. C., Shiekhattar, R. and Shilatifard, A. (2008). *Drosophila* UTX is a histone H3 Lys27 demethylase that colocalizes with the elongating form of RNA polymerase II. *Mol. Cell Biol.* **28**, 1041-1046.
Staehling-Hampton, K., Jackson, P., Clark, M., Brand, A. and Hoffmann, F. (1994). Specificity of bone morphogenetic protein-related factors: cell fate and gene expression changes in *Drosophila* embryos induced by decapentaplegic but not 60A. *Cell. Growth Differ.* **5**, 585-593.
Steffen, P. A. and Ringrose, L. (2014). What are memories made of ? How Polycomb and Trithorax proteins mediate epigenetic memory. *Nat. Rev. Mol. Cell Biol.* **15**, 340-356.
Tie, F., Banerjee, R., Saiakhova, A. R., Howard, B., Monteith, K. E., Scacheri, P. C., Cosgrove, M. S. and Harte, P. J. (2014). Trithorax monomethylates histone H3K4 and interacts directly with CBP to promote H3K27 acetylation and antagonize Polycomb silencing. *Development* **141**, 1129-1139.
Tsai, S.-Y., Chang, Y.-L., Swamy, K. B. S., Chiang, R.-L. and Huang, D.-H. (2016). GAGA factor, a positive regulator of global gene expression, modulates transcriptional pausing and organization of upstream nucleosomes. *Epigenetics Chromatin.* **9**, 1-20.
Venkatesh, S. and Workman, J. L. (2015). Histone exchange, chromatin structure and the regulation of transcription. *Nat. Rev. Mol. Cell Biol.* **16**, 178-189.
Yang, Z., Yik, J. H. N., Chen, R., He, N., Jang, M. K., Ozato, K. and Zhou, Q. (2005). Recruitment of P-TEFb for stimulation of transcriptional elongation by the bromodomain protein Brd4. *Mol. Cell* **19**, 535-545.
Zhao, K., Hart, C. M. and Laemmli, U. K. (1995). Visualization of chromosomal domains with boundary element-associated factor BEAF-32. *Cell* **81**, 879-889.
Zhou, Q., Li, T. D. and Price, D. H. (2012). RNA polymerase II elongation control. *Annu. Rev. Biochem.* **81**, 119-143.